

# EFFECTS OF MARANGONI CONVECTION ON TRANSIENT DROPLET EVAPORATION IN REDUCED GRAVITY

H. Niazmand, B. D. Shaw, and H. A. Dwyer  
Mechanical, Aeronautical and Materials Engineering Department  
University of California  
Davis, CA 95616

Keywords: Droplet Vaporization, Marangoni, Thermocapillary

## INTRODUCTION

Because of its practical and fundamental importance, droplet vaporization, with its complicating features of surface regression, surface blowing, and transient energy and species diffusion, has been the subject of a large number of experimental, analytical and computational studies over the timespan of several decades. A literature review has revealed, however, that previous studies of droplet gasification have generally neglected effects of surface-tension gradients. The only related study that has been found is that of Higuera and Liñán<sup>1</sup>, which is a linear stability analysis of an unsupported and stationary droplet vaporizing in a hot stagnant atmosphere. Here we present a computational study of the effects of Marangoni (thermocapillary) convection on transient temperature and velocity profiles in octane or methanol droplets vaporizing in a hot environment. Large and small droplets (initial diameters of 2 mm and 100  $\mu\text{m}$ ) are considered, and gravity is neglected. The large-droplet calculations are most applicable to reduced-gravity droplet experiments, while the small-droplet calculations are relevant to practical sprays.

Marangoni convection is induced by surface-tension variations along an interface between two fluids. The surface tension variations are caused by temperature gradients parallel to the interface. Since an interface has negligible thickness, surface-tension gradients must be balanced by viscous shear stresses on either side of the interface. If viscous stresses are large relative to surface-tension gradients, thermocapillary effects may be neglected. However, when viscous stresses and surface-tension gradients are comparable, thermocapillary effects are likely very important; this is the situation encountered in thermocapillary migration of droplets and bubbles in temperature gradients. Studies of thermocapillary migration have typically not considered the effects of phase changes, surface regression, surface blowing, or transient energy and species diffusion.

Estimates of the importance of capillary effects on droplet vaporization may be made by considering a droplet of radius  $r$  moving with the speed  $U_\infty$  relative to a gaseous environment. An average shear stress acting on the droplet from the gas side may be defined as  $\rho_\infty U_\infty^2 C_D/2$ , where  $\rho_\infty$  is the ambient gas density and  $C_D$  the drag coefficient. This shear stress will induce convection in the droplet interior. A temperature gradient along the liquid surface will produce an average surface-tension gradient  $\Delta\sigma/r$  ( $\sigma$  is surface tension) that will be balanced by surface shear stresses in the gas and liquid phases. We may characterize  $\Delta\sigma$  as  $\sigma_T \Delta T$ , where  $T$  is temperature,  $\sigma_T = |\partial\sigma/\partial T|$ , and  $\Delta T$  the temperature difference from one side of the droplet to the other. Surface tension gradients will not significantly affect liquid convection processes if  $\Delta\sigma/r$  is significantly less than  $\rho_\infty U_\infty^2 C_D/2$ . In terms of temperature differences, thermocapillary effects should be small if  $\Delta T \ll (\rho_\infty U_\infty^2 C_D/\sigma_T)$ . We may introduce the droplet Reynolds number  $Re = 2rU_\infty\rho_\infty/\mu_\infty$ , where  $\mu_\infty$  is the ambient viscosity, to yield  $\Delta T \ll C_D\mu_\infty^2 Re^2/(4r\sigma_T\rho_\infty)$ . Consider a 2 mm diameter hydrocarbon droplet in 1000 K air at 1 atm. If  $Re = 10$ ,  $C_D = 1$ , and  $\sigma_T = 10^{-4} \text{ N/(m}^2\text{K)}$  (a value appropriate for hydrocarbon or methanol droplets at subcritical conditions<sup>2,3</sup>), we find that  $\Delta T \ll 1 \text{ K}$  is required for surface tension gradients to be negligible. For  $Re = 0.1$  (and  $C_D \approx 24/Re$ ), it is required that  $\Delta T \ll 0.01 \text{ K}$ . Hence, even modest temperature differences may induce significant thermocapillary forces. It is thus desirable to investigate in more detail the effects of capillary

forces on droplets. To this end, a computational model for axisymmetric droplet vaporization, including surface-tension gradients, was developed and is presented below.

## EQUATIONS AND METHODS OF APPROACH

In this paper we started from the low Mach number model of the Navier-Stokes equations in control volume form. This model eliminates acoustic waves from the Navier-Stokes equations, and it will not be derived in the present paper. The equations for axisymmetric flow in control volume form are

### Conservation of Mass

$$\frac{\partial}{\partial t} \iiint_V \rho dV + \oint_A \rho \mathbf{V} \cdot d\bar{\mathbf{A}} = 0$$

### Momentum Equations

$$\iiint_V \rho \left[ \frac{\partial}{\partial t} \mathbf{u} + \mathbf{V} \cdot \nabla \mathbf{u} \right] dV = - \oint_A P \bar{\mathbf{e}}_r \cdot d\bar{\mathbf{A}} + \oint_A \bar{\boldsymbol{\tau}} \cdot d\bar{\mathbf{A}}$$

$$\iiint_V \rho \left[ \frac{\partial}{\partial t} \mathbf{v} + \mathbf{V} \cdot \nabla \mathbf{v} \right] dV = - \oint_A P \bar{\mathbf{e}}_\theta \cdot d\bar{\mathbf{A}} + \oint_A \bar{\boldsymbol{\tau}} \cdot d\bar{\mathbf{A}}$$

### Thermal Energy Equation

$$\iiint_V \rho C_p \left[ \frac{\partial T}{\partial t} + \mathbf{V} \cdot \nabla T \right] dV = \oint_A \lambda \nabla T \cdot d\bar{\mathbf{A}} - \iiint_V \rho \sum_{k=1}^K Y_k C_{p,k} \mathbf{V}_k \cdot \nabla T dV$$

### Species Transport Equations

$$\iiint_V \rho \left[ \frac{\partial Y_i}{\partial t} + \mathbf{V} \cdot \nabla Y_i \right] dV = \oint_A \rho D_i \nabla Y_i \cdot d\bar{\mathbf{A}}$$

### Equation of State

$$P_T = \rho R T$$

where the following notation has been employed:  $\rho$  - is density;  $\mathbf{V}$  - fluid velocity;  $T$  - temperature;  $Y_i$  - mass fraction of species  $i$ ; and  $\bar{\boldsymbol{\tau}}$  is the stress tensor in the fluid. The thermodynamic and transport properties for the gas and liquid have been obtained from Refs. [4-6]. At the interface location between the gas and liquid phases the conditions of continuity of heat flux, mass flux and tangential velocity have been employed, and the equilibrium condition of the Clausius-Clapeyron equation was used to determine the concentration of the liquid components in the gas phase at the interface. Tangential viscous stresses and surface-tension gradients were appropriately balanced at the interface. In addition, gravitational forces were assumed to be negligible.

The above system of equations has been solved numerically with a time accurate method, and with the use of a predictor/corrector method developed previously<sup>7</sup>. In general the addition of surface tension gradients has not caused any explicit change in the numerical methods; however the large surface velocities and gradients generated by surface tension effects have caused a need for smaller time steps to properly resolve the surface phenomena in time. The numerical calculations have been started from a uniform constant velocity initial condition in the gas, and a uniform zero velocity condition in the liquid. This condition, which is typical of droplet injection, causes a rapid buildup of the surface velocities as will be seen in the results section of the paper.

## RESULTS

Calculations were performed for octane or methanol droplets in air at 1 atm. Initial droplet diameters and temperatures were taken in all cases to be 2 mm or 100  $\mu\text{m}$ , and 300 K, respectively. Initial droplet Reynolds numbers of 0.1 and 10 were considered. For the  $\text{Re} = 10$  calculations, vaporization in a 1000 K environment was allowed and the droplet-gas relative velocity was held constant. For  $\text{Re} = 0.1$  vaporization in a 400 K environment was neglected, though droplets slowed down from drag.

Figure 1 shows the transient droplet surface velocity profiles for octane droplets (initially 2 mm) when surface-tension gradients are neglected. (Figures 1 and 2 are three-dimensional plots, with the height above a point in the "time-angle" plane representing the ratio  $U/U_\infty$ , where  $U_\infty$  is the local interface velocity). As would normally be expected, the surface velocities initially rapidly increase and then approach a steady-state condition. In Fig. 2, the same conditions are assumed, except that here thermocapillary effects are allowed. It is evident that that surface velocities are much larger in this case, especially near the beginning of the vaporization history. In each figure, the maximum time plotted is for the gas-phase time scale  $\tau_g = \eta_{\infty}/(\rho_{\infty}r_0^2) = 24.86$ , where  $r_0$  is the initial droplet radius. In Fig. 1, the largest velocity ratio is  $U/U_\infty = 0.036$ , while in Fig. 2 the largest velocity ratio is  $U/U_\infty = 0.086$ .

Figures 3 and 4 show comparisons of droplet temperature profiles at  $\tau_g = 24.86$  for octane and methanol droplets initially 2 mm in diameter. In each figure, the top half shows droplet isotherms when surface-tension gradients are accounted for (case 1), while the bottom half shows droplet isotherms when surface-tension gradients are neglected (case 2). The maximum and minimum temperatures for the isotherms drawn are listed in the figures. For each plot, the temperature difference between each isotherm is the same, though isotherm temperature differences vary between plots. For both fuels, thermocapillary forces significantly affect temperature fields.

Figures 5 and 6 show surface temperature profiles for octane droplets initially 2mm and 100  $\mu\text{m}$  in diameter, respectively, at  $\tau_g = 24.86$ . Cases 1 and 2 correspond to vaporization with and without surface-tension gradients, respectively. In these figures, it is evident that allowing for thermocapillary effects significantly reduces surface temperature variations, especially for larger droplets. In essence, thermocapillary forces act to smooth out temperature gradients by inducing convective flows. Even though surface temperature variations are significantly reduced by thermocapillary effects, the associated thermocapillary flows are still very important. For example, Figs. 7 and 8 show the droplet surface velocity profiles (cases 1 and 2 are as defined above) for the same times listed for Figs. 5 and 6. Again, it is evident that thermocapillary effects significantly affect the velocity profiles. What is especially notable, though, is the prediction that surface-tension gradients tend to decrease droplet surface velocities. The reason for this can be inferred from Figs. 5 and 6, where it can be seen that, at the time shown, the octane droplets are coolest near the stagnation point (angular position of zero). Thermocapillary effects thus strongly oppose gas-phase shear stresses. As a result, surface-tension gradients significantly inhibit droplet internal convection (see also Figs. 3 and 4).

Figure 9 (which is to be interpreted in the same way as Figs 1 and 2) shows transient surface velocity profiles (the maximum time plotted is  $\tau_g = 23.52$ ), while Fig. 10 gives surface velocity profiles at  $\tau_g = 23.52$  for nonvaporizing 2 mm octane droplets subjected to heating in a 400 K environment. These calculations were done for an initial  $\text{Re}$  of 0.1 (the droplet velocity was allowed to decay from drag). Surface-tension gradients were allowed for the results given in Fig. 9. In Fig. 10, results are presented both including and neglecting thermocapillary effects (cases 1 and 2, respectively). A striking feature of Fig. 9 is the oscillatory nature of the velocity profiles. The maximum velocity ratio in Fig. 9 is  $U/U_\infty = 0.126$ . In Fig. 10, it is evident that thermocapillary forces significantly affect velocity profiles; even at this low  $\text{Re}$ , small surface temperature variations produce appreciable effects.

## SUMMARY AND CONCLUSIONS

The calculations presented here demonstrate that thermocapillary effects may significantly influence droplet vaporization, especially during the early periods of a droplet's lifetime. Further work is required to more clearly quantify the effects of capillary forces (from temperature and/or composition variations along a droplet's surface) on droplet gasification phenomena.

## ACKNOWLEDGEMENT

Financial support from NASA and the Daimler-Benz Corporation is gratefully acknowledged.

## REFERENCES

1. Higuera, F. J. and Liñán, A., *Prog. Astro. Aero.* 105: p. 217 (1985).
2. Vargaftik, N. B., *Handbook of Physical Properties of Liquids and Gases*, 2nd ed., Hemisphere (1975).
3. Weast, R. C., *CRC Handbook of Chemistry and Physics*, 65th ed., CRC Press (1984).
4. Kee, R.J., Rupley, F.M., and Miller, J.A.: "Chemkin II: A Fortran Chemical Kinetics Package for the Analysis of Gas-Phase Chemical Kinetics", Sandia National Laboratories Report SAND89-8009 (1990).
5. Kee, R.J., Dixon Lewis, G., Warnitz, J., Coltrin, M.E. and Miller, J.A.: "A Fortran Computer Code Package for the Evaluation of Gas Phase Multicomponent Transport Properties", Sandia National Laboratories Report SAND86-8246 (1986).
6. Reid, R. C., Prausnitz, J. M., and Poling, B. E., *The Properties of Gases and Liquids*, 4th ed., McGraw-Hill (1987).
7. Dwyer, H.A., *Prog. Energy Combust. Sci.* 15, p. 131 (1989).

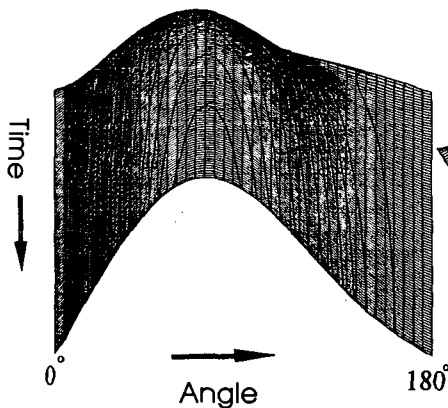


Figure 1. Surface velocity history for a vaporizing octane droplet without thermocapillary effects.

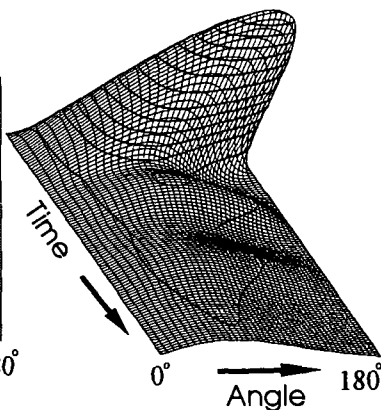
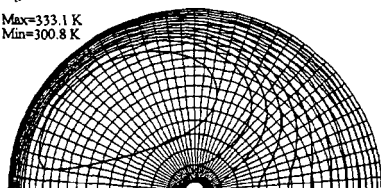


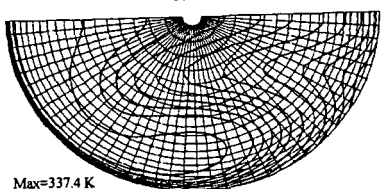
Figure 2. Surface velocity history for a vaporizing octane droplet with thermocapillary effects.

Max=333.1 K  
Min=300.8 K



Case 1

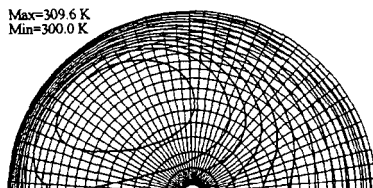
Case 2



Max=337.4 K  
min=300.9 K

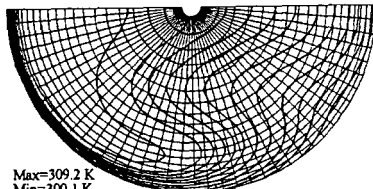
Figure 3. Interior temperature profiles of a vaporizing octane droplet with and without surface tension gradients.

Max=309.6 K  
Min=300.0 K



Case 1

Case 2



Max=309.2 K  
Min=300.1 K

Figure 4. Interior temperature profiles of a vaporizing methanol droplet with and without surface tension gradients.

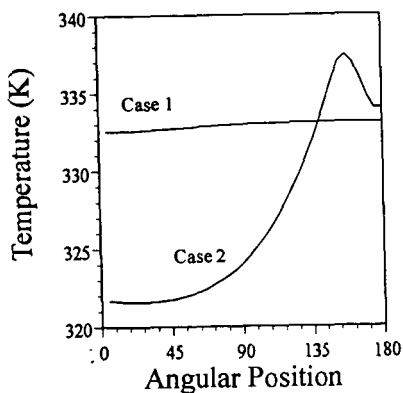


Figure 5. Comparison of surface temperature profiles of a vaporizing octane droplet.

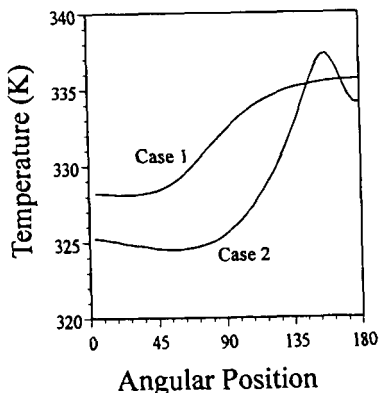


Figure 6. Comparison of surface temperature profiles of a vaporizing small octane droplet.

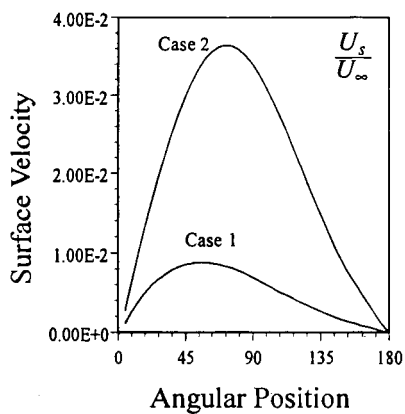


Figure 7. Comparison of surface velocity profiles of a vaporizing octane droplet.

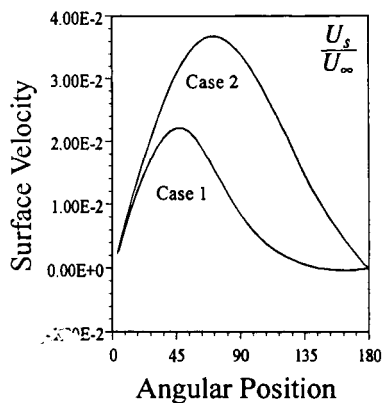


Figure 8. Comparison of surface velocity profiles of a vaporizing small octane droplet.

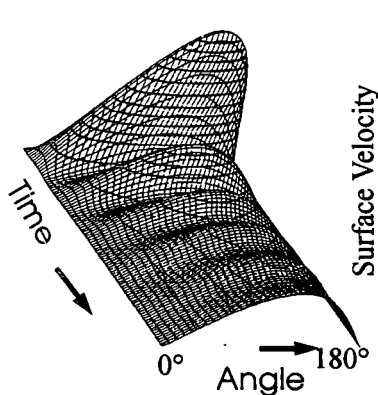


Figure 9. Surface velocity history of a nonvaporizing octane droplet at low Reynolds number with surface tension gradients.

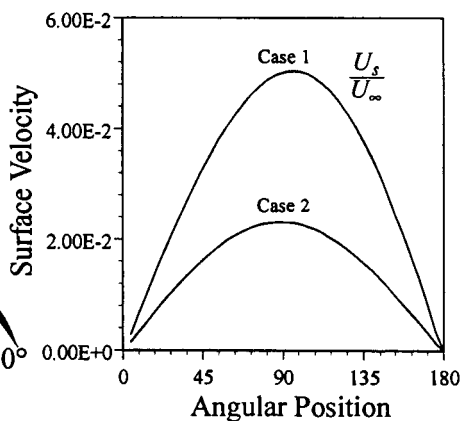


Figure 10. Comparison of surface velocity of an octane droplet at low Reynolds number.